MycoKeys 107: 249–272 (2024)
DOI: 10.3897/mycokeys.107.126139

Research Article

Three new species of *Cyanosporus* (Polyporales, Basidiomycota) from China

Chao-Ge Wang[1*], Shun Liu[2*], Masoomeh Ghobad-Nejhad[3], Hong-Gao Liu[4], Yu-Cheng Dai[1], Yuan Yuan[1]

1 *State Key Laboratory of Efficient Production of Forest Resources, School of Ecology and Nature Conservation, Beijing Forestry University, Beijing 100083, China*
2 *Institute of Ecology and Key Laboratory for Earth Surface Processes of the Ministry of Education, College of Urban and Environmental Sciences, Peking University, Beijing 100871, China*
3 *Department of Biotechnology, Iranian Research Organization for Science and Technology (IROST), Tehran 3353-5111, Iran*
4 *Yunnan Key Laboratory of Gastrodia and Fungi Symbiotic Biology, Zhaotong University, Zhaotong 657000, China*

Corresponding authors: Yu-Cheng Dai (yuchengdai@bjfu.edu.cn); Yuan Yuan (yuanyuan1018@bjfu.edu.cn)

Abstract

Cyanosporus is a cosmopolitan genus characterized by effused-reflexed to pileate basidiomata with a bluish tint and allantoid to cylindrical basidiospores which are negative to weakly positive in Melzer's reagent and Cotton Blue, causing a brown rot. Three new species of *Cyanosporus*, namely, *C. linzhiensis*, *C. miscanthi* and *C. tabuliformis* are described and illustrated. Phylogenies on *Cyanosporus* are reconstructed with seven loci DNA sequences including ITS, nLSU, nSSU, mtSSU, RPB1, RPB2 and TEF1 based on phylogenetic analyses combined with morphological examination. The description for the new species is given. The main morphological characteristics of all 38 accepted species in *Cyanosporus* are summarized.

Key words: Brown rot, phylogeny, polypore, *Postia*, taxonomy, wood-decaying fungi

OPEN ACCESS

Academic editor: María P. Martín
Received: 24 April 2024
Accepted: 22 July 2024
Published: 9 August 2024

Citation: Wang C-G, Liu S, Ghobad-Nejhad M, Liu H-G, Dai Y-C, Yuan Y (2024) Three new species of *Cyanosporus* (Polyporales, Basidiomycota) from China. MycoKeys 107: 249–272. https://doi.org/10.3897/mycokeys.107.126139

Copyright: © Chao-Ge Wang et al.
This is an open access article distributed under terms of the Creative Commons Attribution License (Attribution 4.0 International – CC BY 4.0).

Introduction

The genus *Cyanosporus* McGinty (Polyporales, Basidiomycota), typified by *C. caesius* (Schrad.) McGinty, was established by Lloyd (1909). It is characterized by annual, resupinate, effused-reflexed to pileate basidiomata; white, cream, bluish gray to pinkish buff pileal surface; white, cream, bluish gray to ash gray pore surface, hyphal system monomitic with generative hyphae clamped, and allantoid to cylindrical basidiospores, thin- to slightly thick-walled, with negative to weakly positive reaction in Melzer's reagent and Cotton Blue, causing a brown rot in decayed wood (Papp 2014; Shen et al. 2019; Liu et al. 2021, 2022).

The type species of *Cyanosporus* (*P. caesius*, basionym: *Boletus caesius*) was previously treated as *Polyporus caesius* (Schrad.) Fr. (Fries 1821) and *Tyromyces caesius* (Schrad.) Murrill (Murrill 1907), the latter name was accepted by some mycologists (Donk 1960; Jahn 1963; Lowe 1975). Subsequently, the species was also transferred into *Spongiporus* Murrill, *Postia* Fr., *Oligoporus* Bref., respectively (David 1980; Jülich 1982; Gilbertson and Ryvarden 1985),

* These authors contributed equally as first authors to this work.

because *Postia* has priority over *Spongiporus* and *Oligoporus*, and *Postia caesia* was widely accepted (Papp 2014).

Cyanosporus species were included in *Postia* Fr. typified by *Postia lactea* (Fr.) P. Karst. Molecular analysis (Ţura et al. 2008; Pildain and Rajchenberg 2012; Ortiz-Santana et al. 2013) clustered the *Postia* species in two clades, one of which included *Postia caesia* (Schrad.) P. Karst. Several studies acknowledged the morphological variability of *P. caesia*, and its closely related taxa referred to as *P. caesia* complex (Ţura et al. 2008; Pildain and Rajchenberg 2012; Papp 2014). Papp (2014) discussed the taxonomic status of the *Postia caesia* complex, and proposed a subgenus, *Postia* subg. *Cyanosporus* (McGinty) V. Papp for including the complex (involved five species: *P. alni*, *P. caesia*, *P. luteocaesia*, *P. mediterraneocaesia*, *P. subcaesia*). Miettinen et al. (2018) studied the *Postia caesia* complex based on phylogenetic and morphological analyses, selected a neotype of *P. caesia* (LY BR-6776 collected from Germany) from type locality and described ten new species in *P. caesia* complex. A recent molecular study on *Postia* s.l. and related genera in Shen et al. (2019), considered *Cyanosporus* and *Postia* were two different genera. Two separate species were addressed in the family Postiaceae (Liu et al. 2023). Morphologically both genera differ by the more or less bluish basidiocarps and weakly cyanophilous basidiospores in *Cyanosporus*, while in *Postia*, basidiocarps lack a blue tint and basidiospores are acyanophilous (Shen et al. 2019; Liu et al. 2021, 2022, 2023).

Up to now, 35 species have been accepted in *Cyanosporus*, 23 of which are distributed in China (Liu et al. 2022). During the studies on Chinese polyporoid fungi causing brown rot, some samples were collected from southwest and northern China that morphologically correspond to *Cyanosporus*. The objective of this study is to confirm the identity of these specimens, through a phylogenetic analysis based on a seven loci dataset (ITS+nLSU+mtSSU+nuSSU+RPB1+RPB2+TEF1), and to describe and illustrate the new species.

Materials and methods

Morphological studies

The studied specimens are deposited in the Fungarium of the Institute of Microbiology, Beijing Forestry University (BJFC). Morphological descriptions are based on field notes and voucher specimens. The microscopic analysis follows Miettinen et al. (2018) and Wu et al. (2022a). Sections were studied at a magnification of up to 1000× using a Nikon Eclipse 80i microscope and phase contrast illumination. Description of microscopic features and measurements was made from slide preparations stained with KOH, Cotton Blue and Melzer's reagent. Basidiospores were measured from sections cut from the tubes. To represent the variation in the size of spores, 5% of measurements were excluded from each end of the range and are given in parentheses. In the description: KOH = 5% potassium hydroxide, IKI = Melzer's reagent, IKI– = neither amyloid nor dextrinoid, CB = Cotton Blue, CB– = acyanophilous in Cotton Blue, L = arithmetic average of spore length, W = arithmetic average of spore width, Q = L/W ratios, and n = number of basidiospores/measured from given number of specimens. Color terms follow Anonymous (1969) and Petersen (1996).

DNA extraction, amplification and sequencing

A CTAB rapid plant genome extraction kit-DN14 (Aidlab Biotechnologies Co., Ltd, Beijing) was used to obtain DNA from dried specimens, followed by the polymerase chain reaction (PCR) according to the manufacturer's instructions with some modifications (Shen et al. 2019; Sun et al. 2020). The internal transcribed spacer (ITS) and large subunit nuclear ribosomal RNA gene (nLSU) were amplified using the primer pairs ITS5/ITS4 and LR0R/LR7 (White et al. 1990; Hopple and Vilgalys 1999) (https://sites.duke.edu/vilgalyslab/rdna_primers_for_fungi/). The small subunit mitochondrial ribosomal DNA (mtSSU) region was amplified with primer pairs MS1 and MS2 (White et al. 1990). The small subunit nuclear ribosomal RNA gene (nSSU) region was amplified with primer pairs NS1 and NS4 (White et al. 1990). Part of TEF1 was amplified with primer pairs EF1-983F and EF1-1567R (Rehner and Buckley 2005). The RPB1 was amplified with primer pairs RPB1-Af and RPB1-Cr (Matheny et al. 2002). The RPB2 was amplified with primer pairs fRPB2-5F and fRPB2-7CR (Matheny 2005).

The PCR procedure for ITS, mtSSU and TEF1 was as follows: initial denaturation at 95 °C for 3 min, followed by 34 cycles at 94 °C for 40 s, 54 °C for ITS, 58 °C for mtSSU, and 54 °C for TEF for 45 s and 72 °C for 1 min, and a final extension of 72 °C for 10 min. The PCR procedure for nLSU and nSSU was as follows: initial denaturation at 94 °C for 1 min, followed by 34 cycles of denaturation at 94 °C for 30 s, annealing at 50 °C for nLSU and 52 °C for nSSU for 1 min and extension at 72 °C for 1.5 min, and a final extension at 72 °C for 10 min. The PCR procedure for RPB1 and RPB2 was initial denaturation at 94 °C for 2 min, followed by 10 cycles at 94 °C for 45 s, 60 °C for 45 s and 72 °C for 1.5 min, then followed by 37 cycles at 94 °C for 45 s, 52 °C for 1 min and 72 °C for 1.5 min, and a final extension of 72 °C. The PCR products were purified and sequenced at the Beijing Genomics Institute (BGI), China, with the same primers as used in PCR. Newly generated sequences were deposited in GenBank. All sequences analysed in this study are listed in Table 1.

Table 1. Species, specimens, and GenBank accession number of sequences used for phylogenetic analyses in this study.

Species	Specimen voucher	Country	GenBank accession NO.						
			ITS	LSU	mtSSU	nrSSU	RPB1	RPB2	TEF1
Amaropostia hainanensis B.K. Cui, L.L. Shen & Y.C. Dai	Cui 13739 (holotype)	China	KX900909	KX900979	KX901053	KX901123	KX901171	KX901223	–
A. stiptica (Pers.) B.K. Cui, L.L. Shen & Y.C. Dai	Cui 10043	China	KX900906	KX900976	KX901046	KX901119	KX901167	KX901219	–
Amylocystis lapponica (Romell) Bondartsev & Singer	HHB-13400	USA	KC585237	KC585059	–	–	–	–	–
A. lapponica	OKM-4418	USA	KC585238	KC585060	–	–	–	–	–
Antrodia serpens (Fr.) P. Karst.	Dai 7465	Luxemburg	KR605813	KR605752	KR606013	KR605913	–	KR610832	KR610742
A. tanakae (Murrill) Spirin & Miettinen	Cui 9743	China	KR605814	KR605753	KR606014	KR605914	–	KR610833	KR610743
Calcipostia guttulata (Sacc.) B.K. Cui, L.L. Shen & Y.C. Dai	Cui 10018	China	KF727432	KJ684978	KX901065	KX901138	KX901181	KX901236	KX901276
C. guttulata	Cui 10028	China	KF727433	KJ684979	KX901066	KX901139	KX901182	KX901237	KX901277

Species	Specimen voucher	Country	GenBank accession NO.						
			ITS	LSU	mtSSU	nrSSU	RPB1	RPB2	TEF1
Cyanosporus alni (Niemelä & Vampola) B.K. Cui, L.L. Shen & Y.C. Dai	H 7019137 (holotype)	Slovakia	MG137026	–	–	–	–	–	–
C. alni	Cui 7185	China	KX900879	KX900949	KX901017	KX901092	KX901155	KX901202	KX901254
C. alni	Dai 14845	Poland	KX900880	KX900950	KX901018	KX901093	KX901156	KX901203	KX901255
C. arbuti (Spirin) B.K. Cui & Shun Liu	Spirin 8327 (holotype)	USA	MG137039	–	–	–	–	–	MG137132
C. auricomus (Spirin & Niemelä) B.K. Cui & Shun Liu	Cui 13518	China	KX900887	KX900957	KX901025	KX901100	–	KX901209	–
C. auricomus	Cui 13519	China	KX900888	KX900958	KX901026	KX901101	–	–	–
C. auricomus	TN 8310 (holotype)	Finland	MG137040	–	–	–	–	–	–
C. bifarius (Spirin) B.K. Cui & Shun Liu	Spirin 6402 (holotype)	Russia	MG137043	–	–	–	–	–	MG137133
C. bifarius	Cui 17534	China	OL423598	OL423608	OL437195	OL423620	OL444985	OL446999	OL444994
C. bifarius	Cui 16277	China	OL423599	OL423609	OL437196	OL423621	OL444986	OL447000	OL444995
C. bubalinus B.K. Cui & Shun Liu	Cui 16976	China	MW182172	MW182225	MW182208	MW182189	MW191547	MW191563	MW191530
C. bubalinus	Cui 16985 (holotype)	China	MW182173	MW182226	MW182209	MW182190	MW191548	MW191564	MW191531
C. caesiosimulans (G.F. Atk.) B.K. Cui & Shun Liu	Spirin 4199	Russia	MG137061	–	–	–	–	–	MG137140
C. caesiosimulans	Miettinen 16976 (holotype)	USA	MG137054	–	–	–	–	–	MG137137
C. caesius (Schrad.) McGinty	Schuster 51 (neotype)	Germany	MG137045	–	–	–	–	–	–
C. caesius	Miettinen 14156	Finland	MG137048	–	–	–	–	–	MG137134
C. caesius	Cui 18630	France	OL423600	OL423610	OL437197	OL423622	–	–	OL444996
C. aff. *caesius*	K 32713	UK	AY599576	–	–	–	–	–	–
C. aff. *caesius*	K 32425	UK	AY599575	–	–	–	–	–	–
C. coeruleivirens (Corner) B.K. Cui, Shun Liu & Y.C. Dai	Miettinen 12214	Indonesia	MG137063	–	–	–	–	–	–
C. coeruleivirens	Dai 19220	China	MW182174	MW182227	MW182210	MW182191	MW191549		MW191532
C. comatus (Miettinen) B.K. Cui & Shun Liu	Miettinen 14755,1 (holotype)	USA	MG137066	–	–	–	–	–	–
C. cyanescens (Miettinen) B.K. Cui & Shun Liu	Miettinen 13602 (holotype)	Finland	MG137067	–	–	–	–	–	MG137142
C. cyanescens	Miettinen 15919.2	Spain	MG137071	–	–	–	–	–	MG137144
C. flavus B.K. Cui & Shun Liu	Cui 18547	China	MW448564	MW448561	–	MW448557	MW452596	MW452599	MW452601
C. flavus	Cui 18562 (holotype)	China	MW448565	MW448562	–	MW448558	MW452597	MW452600	MW452602
C. fusiformis B.K. Cui, L.L. Shen & Y.C. Dai	Cui 10775	China	KX900868	KX900938	KX901006	KX901081	–	KX901191	KX901245
C. fusiformis	Dai 15036 (holotype)	China	KX900867	KX900937	KX901005	KX901080	–	KX901190	KX901244
C. glaucus (Spirin & Miettinen) B.K. Cui & Shun Liu	Spirin 5317	Russia	MG137078	–	–	–	–	–	–

Species	Specimen voucher	Country	GenBank accession NO.						
			ITS	LSU	mtSSU	nrSSU	RPB1	RPB2	TEF1
C. glaucus	Spirin 6580 (holotype)	Russia	MG137081	–	–	–	–	–	MG137145
C. gossypinus (Moug. & Lév.) B.K. Cui & Shun Liu	Rivoire 6658 (topotype)	France	–	–	–	–	–	–	MG137146
C. hirsutus B.K. Cui & Shun Liu	Cui 17083 (holotype)	China	MW182179	MW182233	MW182214	MW182197	MW191554	MW191568	MW191538
C. hirsutus	Cui 17343	China	OL423601	OL423611	OL437198	OL423623	OL444987	OL447001	OL444997
C. hirsutus	Cui 17342	China	OL423602	OL423612	OL437199	OL423624	OL444988	OL447002	OL444998
C. linzhiensis	**Dai 27141**	**China**	**PP479781[a]**	**PP479803[a]**	**PP510196[a]**	**PP488288[a]**	**PP526258[a]**	**PP526267[a]**	–
C. linzhiensis	**Dai 27023 (holotype)**	**China**	**PP479782[a]**	**PP479804[a]**	**PP510197[a]**	**PP488289[a]**	**PP526259[a]**	**PP526268[a]**	–
C. livens (Miettinen & Vlasák) B.K. Cui & Shun Liu	Spirin 8728	USA	MG137090	–	–	–	–	–	MG137150
C. livens	Miettinen 17177 (holotype)	USA	MG137082	–	–	–	–	–	MG137147
C. luteocaesius (A. David) B.K. Cui, L.L. Shen & Y.C. Dai	Rivoire 2605 (topotype)	France	MG137091	–	–	–	–	–	–
C. magnus (Miettinen) B.K. Cui & Shun Liu	Dai 21105	China	OL423603	OL423613	OL437200	OL423625	OL444989	OL447003	OL444999
C. magnus	Cui 16983	China	MW182180	MW182234	MW182215	MW182198	MW191555	MW191569	MW191539
C. magnus	Miettinen 10634 (holotype)	China	KC595944	KC595944	–	–	–	–	MG137151
C. mediterraneocaesius (M. Pieri & B. Rivoire) B.K. Cui, L.L. Shen & Y.C. Dai	LY BR 4274	France	KX900886	–	KX901024	KX901099	–	–	–
C. microporus B.K. Cui, L.L. Shen & Y.C. Dai	Cui 11014 (holotype)	China	KX900878	KX900948	KX901016	KX901091	–	KX901201	–
C. microporus	Dai 11717	China	KX900877	KX900947	KX901015	KX901090	–	KX901200	–
C. miscanthi	**Dai 26684**	**China**	**PP479784[a]**	**PP479806[a]**	**PP510199[a]**	**PP488291[a]**	**PP526261[a]**	**PP526270[a]**	**PP526276[a]**
C. miscanthi	**Dai 26687 (holotype)**	**China**	**PP479786[a]**	**PP479808[a]**	**PP510201[a]**	**PP488293[a]**	**PP526263[a]**	**PP526272[a]**	**PP526277[a]**
C. miscanthi	**Dai 26689**	**China**	**PP479783[a]**	**PP479805[a]**	**PP510198[a]**	**PP488290[a]**	**PP526260[a]**	**PP526269[a]**	**PP526275[a]**
C. miscanthi	**Dai 26695**	**China**	**PP479787[a]**	**PP479809[a]**	**PP510202[a]**	**PP488294[a]**	**PP526264[a]**	**PP526273[a]**	**PP526278[a]**
C. miscanthi	**Dai 26701**	**China**	**PP479785[a]**	**PP479807[a]**	**PP510200[a]**	**PP488292[a]**	**PP526262[a]**	**PP526271[a]**	–
C. nothofagicola B.K. Cui, Shun Liu & Y.C. Dai	Cui 16697 (holotype)	Australia	MW182181	MW182235	MW182216	MW182199	MW191556	MW191570	MW191540
C. nothofagicola	Dai 18765	Australia	MW182182	MW182236	MW182217	MW182200	MW191557	–	MW191541
C. piceicola B.K. Cui, L.L. Shen & Y.C. Dai	Cui 10626 (holotype)	China	KX900862	KX900932	KX901001	KX901075	–	KX901185	–
C. piceicola	Cui 12158	China	KX900866	KX900936	KX901004	KX901079	KX901153	KX901189	KX901243
C. populi (Miettinen) B.K. Cui & Shun Liu	Miettinen 17043 (holotype)	USA	MG137092	–	–	–	–	–	MG137153
C. populi	Cui 17087a	China	MW182183	MW182237	MW182218	MW182201	MW191558	MW191571	MW191542
C. populi	Dai 18934	China	OL423604	OL423614	OL437201	OL423626	OL444990	OL447004	OL445000
C. populi	Cui 17557	China	OL423605	OL423615	OL437202	OL423627	OL444991	OL447005	OL445001
C. rigidus B.K. Cui & Shun Liu	Cui 17032 (holotype)	China	OL423606	OL423617	OL437204	OL423629	OL444993	–	OL445003

Species	Specimen voucher	Country	GenBank accession NO.						
			ITS	LSU	mtSSU	nrSSU	RPB1	RPB2	TEF1
C. simulans (P. Karst.) B.K. Cui & Shun Liu	Miettinen 20422	Finland	MG137110	–	–	–	–	–	MG137160
C. simulans	TN 8846 (holotype)	Finland	MG137103	–	–	–	–	–	–
C. subcaesius (A. David) B.K. Cui, L.L. Shen & Y.C. Dai	JV 0110/24	Czechia	MG137117	–	–	–	–	–	MG137164
C. subcaesius	Alix David 652 (isotype)	France	MG137116	–	–	–	–	–	–
C. subhirsutus B.K. Cui, L.L. Shen & Y.C. Dai	Cui 11330	China	KX900873	KX900943	KX901011	KX901086	–	KX901196	KX901250
C. subhirsutus	Dai 14892 (holotype)	China	KX900871	KX900941	KX901009	KX901084	–	KX901194	KX901248
C. submicroporus B.K. Cui & Shun Liu	Cui 16306	China	MW182184	MW182239	MW182220	MW182203	MW191560	MW191573	MW191544
C. submicroporus	Cui 18156 (holotype)	China	MW182186	MW182241	MW182222	MW182205	–	MW191574	–
C. subungulatus B.K. Cui & Shun Liu	Cui 18046 (holotype)	China	MW448566	MW448563	MW448560	MW448559	MW452598	–	MW452603
C. subungulatus	Zhao 10833	China	MW742586	OL423616	OL437203	OL423628	OL444992	–	OL445002
C. subviridis (Ryvarden & Guzmán) B.K. Cui & Shun Liu	Spirin 8774a	USA	MG137120	–	–	–	–	–	MG137166
C. subviridis	Penttilä 14376	Finland	–	–	–	–	–	–	MG137165
C. tabuliformis	**Dai 26063 (holotype)**	**China**	**PP479788[a]**	**PP479810[a]**	**PP510203[a]**	**PP488295[a]**	**PP526265[a]**	**PP526274[a]**	**PP526279[a]**
C. tabuliformis	**Dai 26066**	**China**	**PP479789[a]**	**PP479811[a]**	**PP510204[a]**	**PP488296[a]**	**PP526266[a]**	**–**	**PP526280[a]**
C. tenuicontextus B.K. Cui & Shun Liu	Cui 16280 (holotype)	China	OL423607	OL423618	OL437205	OL423630	–	–	OL445004
C. tenuicontextus	Zhao 813	China	MG231802	OL423619	OL437206	OL423631	–	–	OL445005
C. tenuis B.K. Cui, Shun Liu & Y.C. Dai	Cui 10788 (holotype)	China	KX900885	KX900955	KX901023	KX901098	KX901161	KX901208	–
C. tenuis	Dai 12974	China	KX900884	KX900954	KX901022	KX901097	KX901160	KX901207	KX901258
C. tricolor B.K. Cui, L.L. Shen & Y.C. Dai	Cui 12233 (holotype)	China	KX900876	KX900946	KX901014	KX901089	–	KX901199	KX901253
C. tricolor	Cui 10790	China	KX900875	KX900945	KX901013	KX901088	–	KX901198	KX901252
C. ungulatus B.K. Cui, L.L. Shen & Y.C. Dai	Cui 10778	China	KX900870	KX900940	KX901008	KX901083	–	KX901193	KX901247
C. ungulatus	Dai 12897 (holotype)	China	KX900869	KX900939	KX901007	KX901082	KX901154	KX901192	KX901246
C. yanae (Miettinen & Kotir.) B.K. Cui & Shun Liu	Kotiranta 27606	Russia	MG137122	–	–	–	–	–	MG137168
C. yanae	Kotiranta 27454 (holotype)	Russia	MG137121	–	–	–	–	–	MG137167
Cystidiopostia hibernica (Berk. & Broome) B.K. Cui, L.L. Shen & Y.C. Dai	Cui 2658	China	KX900905	KX900975	KX901045	KX901118	–	KX901218	–
C. inocybe (A. David & Malençon) B.K. Cui, L.L. Shen & Y.C. Dai	LY BR 3703	France	KX900903	KX900973	KX901044	KX901116	–	–	KX901267

Species	Specimen voucher	Country	GenBank accession NO.						
			ITS	LSU	mtSSU	nrSSU	RPB1	RPB2	TEF1
C. pileata (Parmasto) B.K. Cui, L.L. Shen & Y.C. Dai	Cui 10034	China	KX900908	KX900956	KX901050	KX901122	KX901170	KX901222	KX901269
Fuscopostia duplicate (L.L. Shen, B.K. Cui & Y.C. Dai) B.K. Cui, L.L. Shen & Y.C. Dai	Dai 13411 (holotype)	China	KF699125	KJ684976	KR606027	KR605928	KX901174	KR610845	KR610756
F. fragilis (Fr.) B.K. Cui, L.L. Shen & Y.C. Dai	JV 0610/8	Czechia	JF950573	–	–	–	–	–	–
F. leucomallella (Murrill) B.K. Cui, L.L. Shen & Y.C. Dai	Cui 9599	China	KF699123	KJ684983	KX901056	KX901129	KX901176	KX901228	KX901272
Jahnoporus brachiatus Spirin, Vlasák & Miettinen	X 3232	Russia	KU165781	–	–	–	–	–	–
J. hirtus (Cooke) Nuss	Spinosa 10 X 2014	USA	KU165784	–	–	–	KY949044	–	–
J. oreinus Spirin, Vlasák & Miettinen	X 3241	Russia	KU165785	–	–	–	–	–	–
Oligoporus rennyi (Berk. & Broome) Donk	TN-6645	Finland	KC595929	KC595929	–	–	–	–	–
O. sericeomollis (Romell) Bondartseva	Cui 9870	China	KX900920	KX900990	KX901068	KX901141	KX901184	–	–
Osteina obducta (Berk.) Donk	Cui 10074	China	KX900924	KX900994	KX901071	KX901144	–	KX901240	–
O. undosa (Peck) Zmitr.	Dai 7105	China	KX900921	KX900991	KX901069	KX901142	–	KX901238	–
Postia amurensis Y.C. Dai & Penttilä	Dai 903 (holotype)	China	KX900901	KX900971	KX901042	–	–	–	–
P. hirsuta L.L. Shen & B.K. Cui	Cui 11237 (holotype)	China	KJ684970	KJ684984	KX901038	KX901113	–	–	KX901266
P. lactea (Fr.) P. Karst.	Cui 12141	China	KX900892	KX900962	KX901029	KX901104	KX901163	KX901211	KX901260
P. lowei (Pilát) Jülich	Cui 9585	China	KX900898	KX900968	KX901035	KX901110	–	–	–
P. ochraceoalba L.L. Shen, B.K. Cui & Y.C. Dai	Cui 10802 (holotype)	China	KM107903	KM107908	KX901041	KX901115	–	KX901216	–
P. sublowei B.K. Cui, L.L. Shen & Y.C. Dai	Cui 9597 (holotype)	China	KX900900	KX900970	KX901037	KX901112	–	–	KX901265
P. tephroleuca (Fr.) Jülich	Dai 12610	Finland	KX900897	KX900967	KX901034	KX901109	KX901166	KX901214	KX901263
Resupinopostia lateritia (Renvall) B.K. Cui, L.L. Shen & Y.C. Dai	Dai 2652	China	KX900913	KX900983	–	–	–	–	–
R. sublateritia B.K. Cui & Shun Liu	Dai 22760	China	OQ476281	OQ476340	OQ476447	OQ476396	OQ506088	OQ511187	OQ511241
Spongiporus balsameus (Peck) A. David	Cui 9835	China	KX900916	KX900986	KX901061	KX901134	–	KX901233	–
S. leucospongia (Cooke & Harkn.) Murrill	JV 0709/123	USA	–	KX900988	KX901064	KX901137	–	–	KX901275
S. floriformis (Quél.) Zmitr.	Cui 10292	China	KM107899	KM107904	KX901058	KX901131	KX901178	KX901230	KX901274

[a] Newly generated sequences in this study.
Bold = new taxa and sequences generated in this study.

Sequence alignment

Sequences generated from this study were aligned with additional sequences downloaded from GenBank using BioEdit (Hall 1999) and ClustalX (Thompson et al. 1997). The final ITS, nLSU, mtSSU, nSSU, RPB1, RPB2 and TEF1 datasets were subsequently aligned using MAFFT v.7 under the E-INS-i strategy with no cost for opening gaps and equal cost for transformations (command line: mafft –genafpair –maxiterate 1000) (Katoh and Standley 2013) and visualized in BioEdit. Alignments were spliced and transformed formats in Mesquite v.3.2. (Maddison and Maddison 2017). Multiple sequence alignments were trimmed by trimAl v.1.2 using the -htmlout-gt 0.8 -st option to deal with gaps when necessary (Capella-Gutierrez et al. 2009).

Phylogenetic analyses

In this study, a seven loci dataset (ITS+LSU+mtSSU+nrSSU+RPB1+RPB2+TEF1) was used to reconstruct the phylogenetic position of the new species. The sequence alignment and the retrieved topology were deposited in TreeBase (http://www.treebase.org), under accession ID: 31280 (Reviewer access URL: http://purl.org/phylo/treebase/phylows/study/TB2:S31280?x-access-code=605c3765137c8814e37dd70c560cb4de&format=html). Sequences of *Antrodia serpens* (Fr.) P. Karst. and *Antrodia tanakae* (Murrill) Spirin & Miettinen, obtained from GenBank, were used as the outgroups (Liu et al. 2021). The phylogenetic analyses followed the approach of Han et al. (2016) and Zhu et al. (2019). Maximum parsimony (MP), Maximum Likelihood (ML), and Bayesian Inference (BI) analyses were performed based on one dataset. The best-fit evolutionary model was selected by Akaike Information Criterion (AIC) in MrModeltest 2.2 (Nylander 2004) after scoring 24 models of evolution in PAUP* version 4.0b10 (Swofford 2002).

The MP topology and bootstrap values (MP-BS) obtained from 1000 replicates were computed in PAUP* version 4.0b10 (Swofford 2002). All characters were equally weighted, and gaps were treated as missing. Trees were inferred using the heuristic search option with TBR branch swapping and 1000 random sequence additions. Maxtrees were set to 5,000 branches of zero length were collapsed, and all parsimonious trees were saved. Descriptive tree statistics tree length (TL), composite consistency index (CI), retention index (RI), rescaled consistency index (RC), and homoplasy index (HI) were calculated for each maximum parsimonious tree (MPT) generated. Sequences were also analysed using Maximum Likelihood (ML) with RAxML-HPC2 through the CIPRES Science Gateway (Miller et al. 2010). Branch support (BT) for ML analysis was determined by 1 000 bootstrap replicates. Bayesian phylogenetic inference and Bayesian Posterior Probabilities (BPP) were computed with MrBayes 3.1.2 (Ronquist and Huelsenbeck 2003). Four Markov chains were run for 3.5 M generations until the split deviation frequency value was less than 0.01, and trees were sampled every 100 generations. The first 25% of the sampled trees were discarded as burn-in and the remaining ones were used to reconstruct a majority rule consensus and calculate Bayesian Posterior Probabilities (BPP) of the clades. All trees were viewed in FigTree v. 1.4.3 (http://tree.bio.ed.ac.uk/software/figtree/). Branches that received bootstrap support MP ≥ 75%,

ML ≥ 75%, and BPP ≥ 0.95 were considered as significantly supported. The MP and ML bootstrap supports ≥ 50% and BBP ≥ 0.90 are presented on topologies from ML analysis, respectively.

Results

Molecular phylogeny

The combined seven loci dataset (ITS+LSU+mtSSU+nrSSU+RPB1+RPB2+TEF1) included sequences from 115 samples representing 68 species. The dataset had an aligned length of 5639 characters, of which 3800 (56%) characters are constant, 345 (9%) are variable and parsimony-uninformative and 1494 (35%) are parsimony informative. Maximum parsimony analysis yielded eleven equally-parsimonious tree (TL = 6767, CI = 0.414, RI = 0.701, RC = 0.290, HI = 0.586). The phylogenetic reconstruction performed with Maximum Likelihood (ML) and Bayesian Inference (BI) analyses showed similar topology and few differences in statistical support. The best model-fit applied in the Bayesian analysis was GTR+I+G, lset nst = 4, rates = invgamma, and prset statefreqpr = dirichlet (1, 1, 1, 1). Bayesian analysis resulted in a nearly congruent topology with an average standard deviation of split frequencies = 0.008647 to ML analysis, and thus only the ML tree is provided (Fig. 1). The phylogeny (Fig. 1) confirmed *Cyanosporus* and *Postia* as two independent and closely related clades with full support (100% MP, 100% ML, 1.00 BPP). Sequences of three new species, viz. *C. linzhiensis*, *C. miscanthi*, *C. tabuliformis*, were placed in three fully supported and independent lineages in *Cyanosporus* clade (Fig. 1). Though the *Cyanosporus* clade formed two subclades, the supports were at a very weak rate and species in the two subclades share similar characteristics. So the morphological characters cannot explain this separation.

Taxonomy

The main morphological characteristics of the accepted species in *Cyanosporus* are provided in Table 2.

Cyanosporus linzhiensis **Y.C. Dai, Chao G. Wang, Yuan Yuan & Ghobad-Nejhad, sp. nov.**

MycoBank No: 853174

Figs 2, 3

Holotype. China. • Xizang Autonomous Region: Nyingchi, Zayü County, 27 Oct. 2023, on fallen branch of *Pinus yunnanensis*, Dai 27023 (BJFC 044575, GenBank: ITS PP479782, LSU PP479804, mtSSU PP510197, nrSSU PP488289, RPB1 PP526259, RPB2 PP526268).

Etymology. In reference to the species being found in Linzhi (Nyingchi) of Xizang Autonomous Region, southwest China.

Diagnosis. *Cyanosporus linzhiensis* is characterized by their pileate basidiomata with a bluish tint and azonate pileal surface when fresh and dry, white to pale bluish gray pore surface when fresh, pores angular to irregular, 5–6 per mm, cystidioles fusoid and basidiospores allantoid, 4–5 × 1.2–1.5 µm.

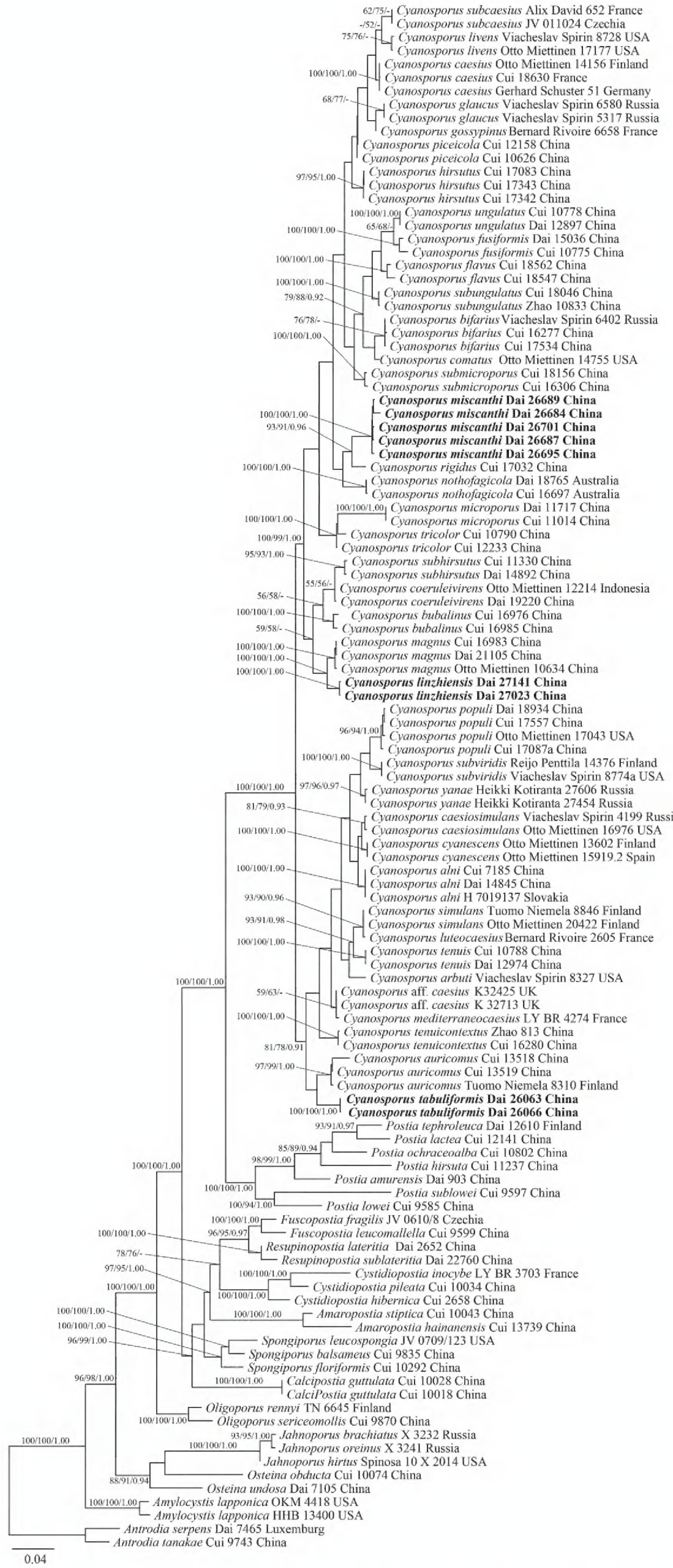
62/75/- Cyanosporus subcaesius Alix David 652 France
-/52/- Cyanosporus subcaesius JV 011024 Czechia
75/76/- Cyanosporus livens Viacheslav Spirin 8728 USA
Cyanosporus livens Otto Miettinen 17177 USA
Cyanosporus caesius Otto Miettinen 14156 Finland
100/100/1.00 Cyanosporus caesius Cui 18630 France
Cyanosporus caesius Gerhard Schuster 51 Germany
68/77/- Cyanosporus glaucus Viacheslav Spirin 6580 Russia
Cyanosporus glaucus Viacheslav Spirin 5317 Russia
Cyanosporus gossypinus Bernard Rivoire 6658 France
Cyanosporus piceicola Cui 12158 China
Cyanosporus piceicola Cui 10626 China
97/95/1.00 Cyanosporus hirsutus Cui 17083 China
Cyanosporus hirsutus Cui 17343 China
Cyanosporus hirsutus Cui 17342 China
100/100/1.00 Cyanosporus ungulatus Cui 10778 China
65/68/- Cyanosporus ungulatus Dai 12897 China
100/100/1.00 Cyanosporus fusiformis Dai 15036 China
Cyanosporus fusiformis Cui 10775 China
100/100/1.00 Cyanosporus flavus Cui 18562 China
Cyanosporus flavus Cui 18547 China
100/100/1.00 Cyanosporus subungulatus Cui 18046 China
79/88/0.92 Cyanosporus subungulatus Zhao 10833 China
76/78/- Cyanosporus bifarius Viacheslav Spirin 6402 Russia
100/100/1.00 Cyanosporus bifarius Cui 16277 China
Cyanosporus bifarius Cui 17534 China
Cyanosporus comatus Otto Miettinen 14755 USA
Cyanosporus submicroporus Cui 18156 China
Cyanosporus submicroporus Cui 16306 China
Cyanosporus miscanthi Dai 26689 China
100/100/1.00 **Cyanosporus miscanthi Dai 26684 China**
93/91/0.96 **Cyanosporus miscanthi Dai 26701 China**
Cyanosporus miscanthi Dai 26687 China
Cyanosporus miscanthi Dai 26695 China
100/100/1.00 Cyanosporus rigidus Cui 17032 China
Cyanosporus nothofagicola Dai 18765 Australia
Cyanosporus nothofagicola Cui 16697 Australia
100/100/1.00 Cyanosporus microporus Dai 11717 China
Cyanosporus microporus Cui 11014 China
100/100/1.00 Cyanosporus tricolor Cui 10790 China
100/99/1.00 Cyanosporus tricolor Cui 12233 China
95/93/1.00 Cyanosporus subhirsutus Cui 11330 China
Cyanosporus subhirsutus Dai 14892 China
55/56/- Cyanosporus coeruleivirens Otto Miettinen 12214 Indonesia
56/58/- Cyanosporus coeruleivirens Dai 19220 China
100/100/1.00 Cyanosporus bubalinus Cui 16976 China
59/58/- Cyanosporus bubalinus Cui 16985 China
100/100/1.00 Cyanosporus magnus Cui 16983 China
100/100/1.00 Cyanosporus magnus Dai 21105 China
100/100/1.00 Cyanosporus magnus Otto Miettinen 10634 China
Cyanosporus linzhiensis Dai 27141 China
Cyanosporus linzhiensis Dai 27023 China
Cyanosporus populi Dai 18934 China
96/94/1.00 Cyanosporus populi Cui 17557 China
Cyanosporus populi Otto Miettinen 17043 USA
Cyanosporus populi Cui 17087a China
100/100/1.00 Cyanosporus subviridis Reijo Penttila 14376 Finland
Cyanosporus subviridis Viacheslav Spirin 8774a USA
100/100/1.00 97/96/0.97 Cyanosporus yanae Heikki Kotiranta 27606 Russia
Cyanosporus yanae Heikki Kotiranta 27454 Russia
81/79/0.93 Cyanosporus caesiosimulans Viacheslav Spirin 4199 Russia
Cyanosporus caesiosimulans Otto Miettinen 16976 USA
100/100/1.00 Cyanosporus cyanescens Otto Miettinen 13602 Finland
Cyanosporus cyanescens Otto Miettinen 15919.2 Spain
100/100/1.00 Cyanosporus alni Cui 7185 China
Cyanosporus alni Dai 14845 China
Cyanosporus alni H 7019137 Slovakia
93/90/0.96 Cyanosporus simulans Tuomo Niemela 8846 Finland
93/91/0.98 Cyanosporus simulans Otto Miettinen 20422 Finland
Cyanosporus luteocaesius Bernard Rivoire 2605 France
100/100/1.00 Cyanosporus tenuis Cui 10788 China
Cyanosporus tenuis Dai 12974 China
Cyanosporus arbuti Viacheslav Spirin 8327 USA
100/100/1.00 Cyanosporus aff. caesius K32425 UK
59/63/- Cyanosporus aff. caesius K 32713 UK
Cyanosporus mediterraneocaesius LY BR 4274 France
100/100/1.00 Cyanosporus tenuicontextus Zhao 813 China
81/78/0.91 Cyanosporus tenuicontextus Cui 16280 China
Cyanosporus auricomus Cui 13518 China
97/99/1.00 Cyanosporus auricomus Cui 13519 China
Cyanosporus auricomus Tuomo Niemela 8310 Finland
Cyanosporus tabuliformis Dai 26063 China
100/100/1.00 **Cyanosporus tabuliformis Dai 26066 China**
93/91/0.97 Postia tephroleuca Dai 12610 Finland
Postia lactea Cui 12141 China
85/89/0.94 Postia ochraceoalba Cui 10802 China
100/100/1.00 98/99/1.00 Postia hirsuta Cui 11237 China
Postia amurensis Dai 903 China
100/100/1.00 Postia sublowei Cui 9597 China
100/94/1.00 Postia lowei Cui 9585 China
100/100/1.00 Fuscopostia fragilis JV 0610/8 Czechia
96/95/0.97 Fuscopostia leucomallella Cui 9599 China
100/100/1.00 Resupinopostia lateritia Dai 2652 China
78/76/- Resupinopostia sublateritia Dai 22760 China
97/95/1.00 100/100/1.00 Cystidiopostia inocybe LY BR 3703 France
100/100/1.00 Cystidiopostia pileata Cui 10034 China
100/100/1.00 Cystidiopostia hibernica Cui 2658 China
100/100/1.00 Amaropostia stiptica Cui 10043 China
100/100/1.00 Amaropostia hainanensis Cui 13739 China
96/99/1.00 Spongiporus leucospongia JV 0709/123 USA
Spongiporus balsameus Cui 9835 China
Spongiporus floriformis Cui 10292 China
96/98/1.00 100/100/1.00 Calcipostia guttulata Cui 10028 China
CalciPostia guttulata Cui 10018 China
Oligoporus rennyi TN 6645 Finland
100/100/1.00 Oligoporus sericeomollis Cui 9870 China
93/95/1.00 Jahnoporus brachiatus X 3232 Russia
100/100/1.00 100/100/1.00 Jahnoporus oreinus X 3241 Russia
Jahnoporus hirtus Spinosa 10 X 2014 USA
Osteina obducta Cui 10074 China
88/91/0.94 Osteina undosa Dai 7105 China
100/100/1.00 Amylocystis lapponica OKM 4418 USA
Amylocystis lapponica HHB 13400 USA
Antrodia serpens Dai 7465 Luxemburg
Antrodia tanakae Cui 9743 China
0.04

Figure 1. A Maximum Likelihood phylogenetic tree of *Cyanosporus* based on a dataset of ITS+nLSU+mtSSU+nuSSU+RPB1+RPB2+TEF1. ML bootstrap values higher than 50% and Bayesian posterior probabilities values more than 0.90 are shown. New taxa are in bold.

Table 2. The main morphological characteristics of the accepted species in *Cyanosporus*.

Species	Type locality	Basidiomata	Upper surface	Color of poroid surface	Amyloid (greenish in IKI) tramal hyphae	Shape of basidiospores	Size of Basidiospores (µm)	Cyanophilous basidiospores	References
C. alni	Slovakia	Annual, Pileate to rarely effused-reflexed	Cream, ochraceous to brownish with a bluish-grayish tint; velutinate	White to cream, in older and dry specimens with a light bluish-grayish tint	–	Allantoid to very narrow cylindrical	4.4–6 × 1.1–1.3	–	Niemelä et al. (2001); Miettinen et al. (2018)
C. arbuti	USA	Annual, Pileate to effused-reflexed	White to pale cream; glabrous	White to cream, in older and dry specimens with a light bluish-grayish tint	–	Allantoid	4.1–5.1 × 1–1.2	+	Miettinen et al. (2018)
C. auricomus	Finland	Annual, Pileate	White to cream, yellowish to bright yellow, in older specimens with pale to dark ochraceous; hirsute	Bright yellow, green when bruised, then with an ochraceous tint	+	Allantoid	4.4–5.6 × 1.5–1.8	+	Miettinen et al. (2018)
C. bifarius	Russia	Annual, Pileate	Light gray, then with an ochraceous tint; velutinate	White to cream, in older and dry specimens with a light ochraceous tint	–	Allantoid	3.7–4.4 × 1–1.2	+	Miettinen et al. (2018)
C. bubalinus	China	Annual, Pileate	White to cream when fresh, cream to pinkish buff when dry; tomentose	White to cream when fresh, straw yellow to buff when dry	–	Cylindrical, slightly curved	4.3–4.8 × 1.2–1.7	–	Liu et al. (2021)
C. caesiosimulans	USA	Annual, Pileate to effused-reflexed	White to cream, then grayish to pale ochraceous with very rarely with bluish flecks or faint zones; glabrous	White to cream, in older and dry specimens with a light bluish-grayish tint	–	Allantoid	4.2–5.5 × 1.1–1.4	+	Miettinen et al. (2018)
C. caesius	Germany	Annual, Pileate to effused-reflexed	Grayish to bluish when fresh, blue when bruised; hirsute	White to pale gray when fresh, bluish when bruised	+	Cylindrical to allantoid	4.5–6 × 1.5–2	+	Ryvarden and Gilbertson (1994)
C. coeruleivirens	Malaysia	Annual, Pileate	White to bluish green; velutinate	White when fresh, bluish green when bruised	–	Allantoid	4–5 × 1–1.3	+	Corner (1989)
C. comatus	USA	Annual, Pileate to effused-reflexed	Cream to pale ochraceous; velutinate	Cream, in older and dry specimens with a bluish-grayish tint	–	Allantoid	4.1–4.9 × 1.1–1.3	+	Miettinen et al. (2018)
C. cyanescens	Finland	Annual, Pileate to reraly effused-reflexed	White to pale ochraceous, then pale ochraceous, rarely with a bluish-grayish tint; glabrous	White to cream, in older and dry specimens with a light bluish-grayish tint	–	Allantoid	4.7–6.1 × 1.1–1.6	+	Miettinen et al. (2018)
C. flavus	China	Annual, Pileate	Ash-gray to light vinaceous gray when fresh, pale mouse-gray to mouse-gray when dry; hirsute	White to cream when fresh, buff to lemon-chrome when dry	–	Slim allantoid	4.6–5.2 × 0.8–1.3	–	Liu et al. (2022)
C. fusiformis	China	Annual, Pileate to effused-reflexed	White to cream, with a blue tint at the center when fresh, vinaceous gray to dark gray when dry; tomentose	White when fresh, buff to clay buff when dry	–	Slim allantoid	4.5–5.2 × 0.8–1.1	–	Shen et al. (2019)
C. glaucus	Russia	Annual, Pileate	Grayish, plumbeous to bluish gray or grayish-brown; hirsute	White to cream when fresh, in older and dry specimens with a light bluish-grayish tint	+	Allantoid	4.1–5.4 × 1.1–1.5	+	Miettinen et al. 2018

Species	Type locality	Basidiomata	Upper surface	Color of poroid surface	Amyloid (greenish in IKI) tramal hyphae	Shape of basidiospores	Size of Basidiospores (µm)	Cyanophilous basidiospores	References
C. gossypinus	France	Annual, Pileate	Cream to light gray; glabrous	Cream to bluish-grayish	–	Cylindrical to allantoid	4.1–5.1 × 1.2–1.7	+	Miettinen et al. (2018)
C. hirsutus	China	Annual, Pileate	Ash-gray to light grayish brown with bluish gray zones when fresh, grayish to grayish brown when dry; hirsute	Cream when fresh, straw yellow to olivaceous buff when dry	–	Cylindrical, slightly curved	4–4.7 × 1.2–1.5	–	Liu et al. (2021)
C. linzhiensis	China	Annual, pileate	White with a blue tint when fresh, becoming white to pinkish buff when dry; velutinate	White to pale bluish gray when fresh, pinkish buff to honey yellow and with a blue tint when dry	–	Allantoid	4–5 × 1.2–1.5	–	This study
C. livens	USA	Annual, Pileate	Cream, plumbeous to bluish gray to ochraceous; velutinate	Cream, in older and dry specimens with a light bluish-grayish tint	–	Cylindrical to allantoid	4.1–5.7 × 1.1–1.5	+	Miettinen et al. (2018)
C. luteocaesius	France	Annual, resupinate to effused-reflexed	White to yellow when fresh, brownish when dry; tomentose	Yellow when fresh, with a light bluish tint when bruised	+	Allantoid	5–6 × 2	+	Ryvarden and Gilbertson (1994)
C. magnus	China	Annual, Pileate	White when fresh, cream to light grayish and ochraceous when dry; velutinate	White when fresh, ochraceous with a bluish tint when dry	–	Allantoid	3.6–4.4 × 1–1.2	+	Miettinen et al. (2018)
C. mediterraneocaesius	France	Annual, effused-reflexed to resupinate	White to cream or pale ochraceous; velutinate	White to cream, in older and dry specimens pale ochraceous, with a light bluish-grayish tint	–	Cylindrical to allantoid	4.2–5.8 × 1.3–1.7	+	Miettinen et al. (2018)
C. microporus	China	Annual, Pileate	White to cream with blue tint when fresh, cream to pinkish-buff when dry; velutinate	White when fresh, bluish when bruised, cream to buff when dry	–	Allantoid	4.5–4.9 × 1–1.2	–	Shen et al. (2019)
C. miscanthi	China	Annual, Pileate to effused-reflexed	White to pale bluish gray when fresh and dry; velutinate	White to pale bluish gray when fresh, bluish gray to ash gray when dry	–	Cylindrical to allantoid	4–5 × 1.5–2	–	This study
C. nothofagicola	Australia	Annual, Pileate to effused-reflexed	Buff to olivaceous buff when fresh, pale mouse gray to buff yellow when dry; tomentose	White to cream when fresh, cream to buff yellow when dry	–	Cylindrical to allantoid	3.8–5 × 1–1.7	–	Liu et al. (2021)
C. piceicola	China	Annual, Pileate	Cream to clay buff, with bluish gray zones when fresh, light grayish-brown when dry; velutinate	White with a bluish tint when fresh, cream when dry	–	Allantoid	4–4.5 × 0.9–1.3	–	Shen et al. (2019)
C. populi	USA	Annual, Pileate to effused-reflexed	White to cream, pale ochraceous to grayish, rarely with bluish flecks or indistinct zones; glabrous	White to cream when fresh, in older and dry specimens with a light bluish-grayish tint	–	Cylindrical to allantoid	4.2–5.6 × 1–1.3	+	Miettinen et al. (2018)
C. rigidus	China	Annual, Pileate	Buff yellow to clay buff when fresh, olivaceous buff to grayish brown when dry; glabrous	White to cream when fresh, buff yellow to pinkish buff when dry	–	Cylindrical to allantoid	3.7–4.2 × 0.9–1.3	–	Liu et al. (2022)
C. simulans	Finland	Annual, effused-reflexed to resupinate	White to cream when fresh, blue, grayish or pale ochraceous when dry; glabrous	White to cream when fresh, in older and dry specimens with a light bluish-grayish tint	+	Cylindrical to allantoid	4.4–6.3 × 1.3–1.8	+	Miettinen et al. (2018)

Species	Type locality	Basidiomata	Upper surface	Color of poroid surface	Amyloid (greenish in IKI) tramal hyphae	Shape of basidiospores	Size of Basidiospores (µm)	Cyanophilous basidiospores	References
C. subcaesius	France	Annual, Pileate to effused-reflexed	White to ochraceous with a slight grayish to bluish tint in spots and streaks; glabrous	White to pale gray	–	Allantoid	4–5 × 1–1.2	–	Ryvarden and Melo (2017)
C. subhirsutus	China	Annual, Pileate	Pale mouse-gray and cream zones when fresh, cream to buff when dry; hirsute	White when fresh, pinkish buff to honey yellow when dry	–	Allantoid	4–4.5 × 0.9–1.3	+	Shen et al. (2019)
C. submicroporus	China	Annual, Pileate	Cream to pinkish buff when fresh, buff to buff yellow when dry; velutinate	White to smoky gray when fresh, buff to olivaceous buff when dry	–	Allantoid	3.6–4.7 × 1–1.3	+	Liu et al. (2021)
C. subungulatus	China	Annual, Pileate	Pale mouse-gray to ash-gray when fresh, dark-gray to mouse-gray when dry; glabrous	White to cream when fresh, cream to pinkish buff when dry	–	Cylindrical to allantoid	4.5–5.2 × 1.1–1.4	–	Liu et al. (2022)
C. subviridis	Mexico	Annual, Pileate	Pale ochraceous, ochraceous to grayish; glabrous	White to cream, in older and dry specimens with a light bluish-grayish tint	–	Cylindrical to allantoid	3.8–4.5 × 1–1.3	+	Miettinen et al. (2018)
C. tabuliformis	China	Annual, pileate	Cream to buff at the base, grayish blue at the margin when fresh, olivaceous buff to ash gray when dry; hirsute	White to sulphur yellow when fresh, cream, pale cinnamon buff to pale mouse-gray when dry	–	Cylindrical to allantoid	4.3–5.5 × 1.5–2	–	This study
C. tenuicontextus	China	Annual, Pileate	Cream to pinkish buff with a little blue tint when fresh, light vinaceous gray to pale mouse-gray when dry; velutinate	White to cream when fresh, pinkish buff to buff when dry	–	Allantoid	3.8–4.3 × 0.8–1.2	–	Liu et al. (2022)
C. tenuis	China	Annual, Pileate to effused-reflexed	Buff to olivaceous buff when fresh, cream to olivaceous buff when dry; tomentose	White to cream when fresh, buff yellow to pinkish buff when dry	–	Cylindrical, slightly curved	4.7–6 × 1.3–2	+	Liu et al. (2021)
C. tricolor	China	Annual, Pileate	Light grayish brown with bluish gray zones when fresh, grayish brown when dry; velutinate	White when fresh, cream to buff when dry	–	Allantoid	4–4.8 × 0.8–1.2	+	Shen et al. (2019)
C. ungulatus	China	Annual, Pileate	Olivaceous buff, pinkish buff, cream to ash-gray and white zones when fresh, slightly darkening when dry; glabrous	White when fresh, cream when dry	–	Allantoid	4.5–5 × 0.9–1.2	–	Shen et al. (2019)
C. yanae	Russia	Annual, effused-reflexed to resupinate	White to cream, pale ochraceous or bluish to deep brown; glabrous	White, with a light to strong bluish-grayish tint	–	Cylindrical to allantoid	4.3–5.8 × 1.2–1.6	+	Miettinen et al. (2018)

Bold = new taxa. Abbreviations used: + = present, – = Absent.

Figure 2. Basidiomata of *Cyanosporus linzhiensis* (Dai 27023, holotype). Scale bar: 1 cm.

Basidiomata annual, pileate, soft and without odor or taste when fresh, becoming soft corky to fragile upon drying; pileus flabelliform, up to 3 cm, 3.5 cm wide and 8 mm thick at the base. Pileal surface white, somewhat with a bluish tint when fresh, becoming white to pinkish buff when dry, velutinate, azonate. Hymenophore white to pale bluish gray when fresh, becoming pinkish buff to honey yellow and with a blue tint upon drying; sterile margin almost absent; pores angular to irregular, 5–6 per mm, with thin dissepiments becoming lacerate. Context white, soft corky, up to 5 mm thick. Tubes concolorous with pore surface, soft corky to fragile when dry, up to 3 mm long. Context and tubes turn dark olive green in KOH.

Hyphal system monomitic; hyphae clamped, hyaline, slightly thick-walled, with a wide lumen, smooth; in the context frequently branched, more or less flexuous, loosely interwoven, 3–5 µm in diam; in the tubes unbranched, straight, subparallel along the tubes, agglutinated, 2–3.5 µm in diam.

Cystidia absent, but cystidioles fusoid are present, thin-walled, 12–13.5 × 3 µm.

Basidia clavate, 9–13 × 4–5 µm, with basal clamp and four sterigmata.

Basidiospores allantoid, 4–5 × 1.2–1.5 µm, L = 4.5 µm, W = 1.4 µm, Q= 3.1–3.5 (n = 60/2), thin-walled, smooth, hyaline, IKI−, CB−.

Type of rot. Brown rot.

Additional specimen examined. China. • Xizang Autonomous Region: Nyingchi, Bomê County, 27 Oct. 2023, on fallen angiosperm trunk, Dai 27141 (BJFC 044575, GenBank: ITS PP479781, LSU PP479803, mtSSU PP510196, nrSSU PP488288, RPB1 PP526258, RPB2 PP526267).

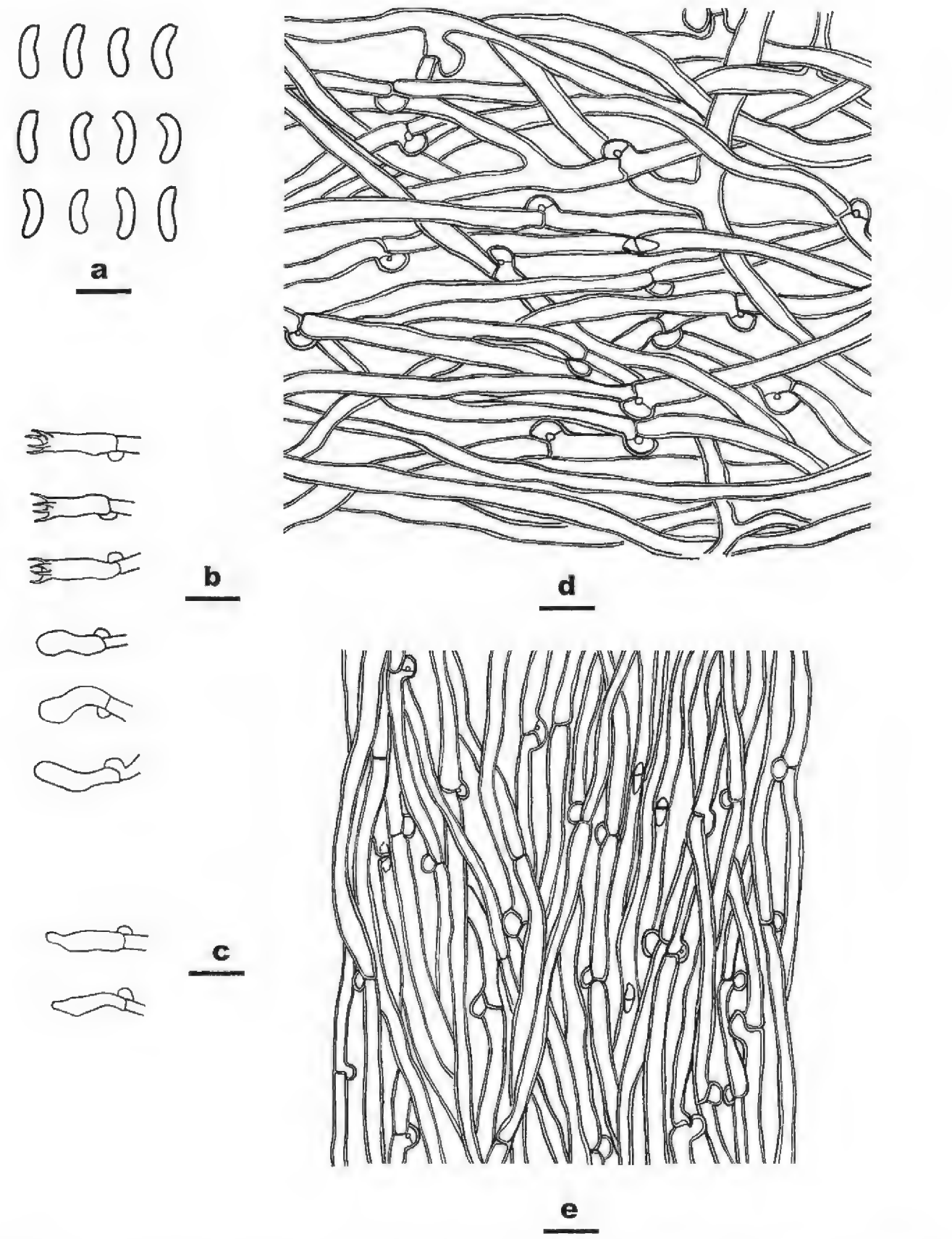

Figure 3. *Cyanosporus linzhiensis* (Dai 27023, holotype,) **A** basidiospores **B** basidia and basidioles **C** cystidioles **D** hyphae from context **E** hyphae from trama. Scale bars: 5 μm (**A**); 10 μm (**B–E**).

Cyanosporus miscanthi **Y.C. Dai, Chao G. Wang, Yuan Yuan & Ghobad-Nejhad, sp. nov.**

MycoBank No: 853175

Figs 4, 5

Holotype. China. • Xizang Autonomous Region: Nyingchi, Medog County, 24 Oct. 2023, on dead *Miscanthus*, Dai 26687 (BJFC 044237, GenBank: ITS PP479786, LSU PP479808, mtSSU PP510201, nrSSU PP488293, RPB1 PP526263, RPB2 PP526272, TEF1 PP526277).

Etymology. In reference to *Miscanthus* the genus where this species was found.

Diagnosis. *Cyanosporus miscanthi* is characterized by effused-reflexed to pileate tiny basidiomata, slightly concentrically zonate pileal surface, white to pale bluish gray pore surface when fresh, angular pores, 7–9 per mm, fusoid cystidioles and cylindrical to allantoid basidiospores, 4–5 × 1.5–2 μm.

Figure 4. Basidiomata of *Cyanosporus miscanthi* (Dai 26687, holotype). Scale bar: 1 cm.

Basidiomata annual, effused-reflexed to pileate, soft and without odor or taste when fresh, becoming fragile to soft corky upon drying, up to 1 cm long and 0.8 cm wide when resupinate; pileus semicircular, projecting up to 0.8 cm, 1.2 cm wide and 1.2 mm thick at the base. Pileal surface white, pale bluish gray to bluish green when fresh and dry, velutinate, slightly concentrically zonate when dry; margin sharp, slightly curved when dry. Hymenophore poroid, white to pale bluish gray when fresh, becoming bluish gray to ash gray when dry; sterile margin almost absent; pores angular, 7–9 per mm; dissepiments thin, entire to slightly lacerate. Context white, soft corky, up to 0.3 mm thick. Tubes concolorous with pore surface, fragile to soft corky when dry, up to 0.9 mm long. Context and tubes turn dark olive green in KOH.

Hyphal system monomitic; hyphae clamped, hyaline, slightly thick-walled, smooth, with a wide lumen, frequently branched, more or less flexuous, in the context loosely interwoven, 3–4.5 µm in diam in the tubes subparallel along the tubes, agglutinated, 2.5–3 µm in diam.

Cystidia absent, but cystidioles fusoid present, thin-walled, 11–15 × 4 µm.

Basidia clavate, 9–13 × 4–5 µm, with four sterigmata and a basal clamp connection.

Basidiospores cylindrical to allantoid, 4–5(–5.5) × 1.5–2 µm, L = 4.2 µm, W = 1.9 µm, Q = 2.2–2.4 (n = 120/4), hyaline, thin-walled, IKI–, CB–.

Type of rot. Brown rot.

Additional specimens examined. China. • Xizang Autonomous Region: Nyingchi, Medog County, 24 Oct. 2023, on dead *Miscanthus*, Dai 26684 (BJFC044234, ITS PP479784, LSU PP479806, mtSSU PP510199, nrSSU PP488291, RPB1 PP526261, RPB2 PP526270, TEF1 PP526276); Dai 26695 (BJFC044245, ITS PP479787, LSU

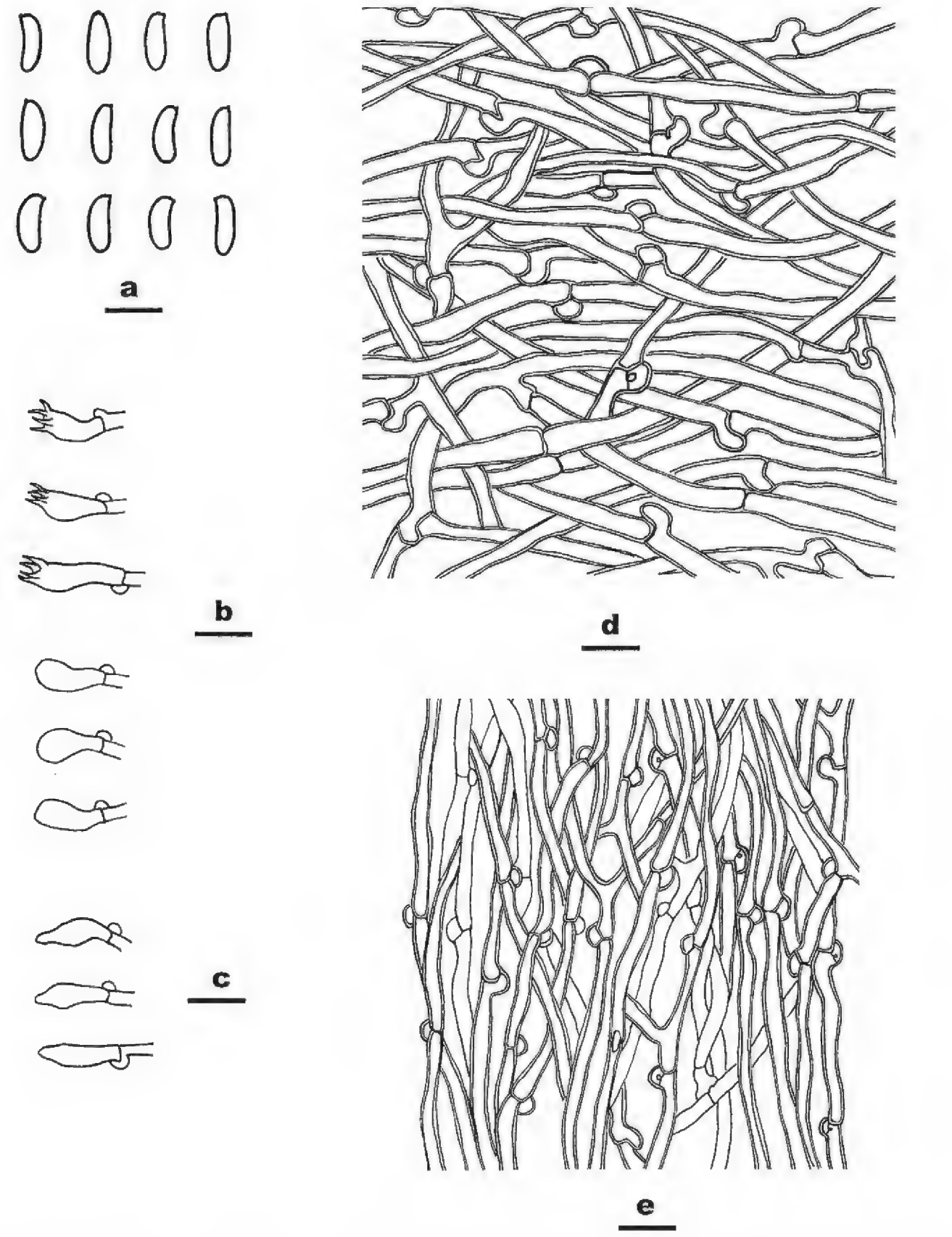

Figure 5. *Cyanosporus miscanthi* (Dai 26687, holotype) **A** basidiospores **B** basidia and basidioles **C** cystidioles **D** hyphae from context **E** hyphae from trama. Scale bars: 5 μm (**A**); 10 μm (**B–E**).

PP479809, mtSSU PP510202, nrSSU PP488294, RPB1 PP526264, RPB2 PP526273, TEF1 PP526278); Dai 26689 (BJFC044239, ITS PP479783, LSU PP479805, mtSSU PP510198, nrSSU PP488290, RPB1 PP526260, RPB2 PP526269, TEF1 PP526275); Dai 26701 (BJFC044251, ITS PP479785, LSU PP479807, mtSSU PP510200, nrSSU PP488292, RPB1 PP526262, RPB2 PP526271).

***Cyanosporus tabuliformis* Y.C. Dai, Chao G. Wang, Yuan Yuan & Ghobad-Nejhad, sp. nov.**

MycoBank No: 853176

Figs 6, 7

Holotype. China. • Shanxi Province: Changzhi, Qinyuan County, Taiyueshan Forest Park, 31 Aug. 2023, on fallen branch of *Pinus tabuliformis*, Dai 26063 (BJFC

043612, Genbank: ITS PP479788, LSU PP479810, mtSSU PP510203, nrSSU PP488295, RPB1 PP526265, RPB2 PP526274, TEF1 PP526279).

Etymology. In reference to the specific epithet of the substrate, *Pinus tabuliformis* in which this species was found.

Diagnosis. *Cyanosporus tabuliformis* is characterized by a pileate basidiomata with cream, buff to grayish blue and hirsute azonate pileal surface when fresh, angular pores, 4–5 per mm, fusoid cystidioles, and cylindrical to allantoid basidiospores, 4.3–5.5 × 1. 5–2 µm.

Basidiomata annual, pileate, soft and without odor or taste when fresh, becoming more or less fragile to corky upon drying. Pileus flabelliform, projecting up to 1.5 cm, 3.5 cm wide and 5 mm thick at the base. Pileal surface cream to buff at the base, grayish blue at the margin when fresh, becoming olivaceous buff to ash gray upon drying, hirsute, azonate when dry; margin blunt. Hymenophore poroid, white to sulphur yellow when fresh, unchanged when bruised, becoming cream, pale cinnamon buff to pale mouse gray upon drying; sterile margin white when fresh, cream to buff when dry, up to 0.2 mm wide; pores angular to irregular, 4–5 per mm, with thin dissepiments, becoming lacerate. Context white, soft corky, up to 2 mm thick. Tubes concolorous with pore surface, fragile to soft corky when dry, up to 3 mm long.

Hyphal system monomitic, hyphae clamped, hyaline, slightly thick-walled with a wide lumen, in the context frequently branched, straight, distinctly interwoven, 3–4 µm in diam; in the tubes rarely branched, more or less flexuous, subparallel along the tubes, agglutinated, 2.8–3.5 µm in diam.

Cystidia absent, but cystidioles fusoid present, 10–12 × 4 µm.

Basidia clavate, 13–16 × 4.5–5 µm, with basal clamp and four sterigmata.

Figure 6. Basidiomata of *Cyanosporus tabuliformis* (Dai 26063, holotype). Scale bar: 1 cm.

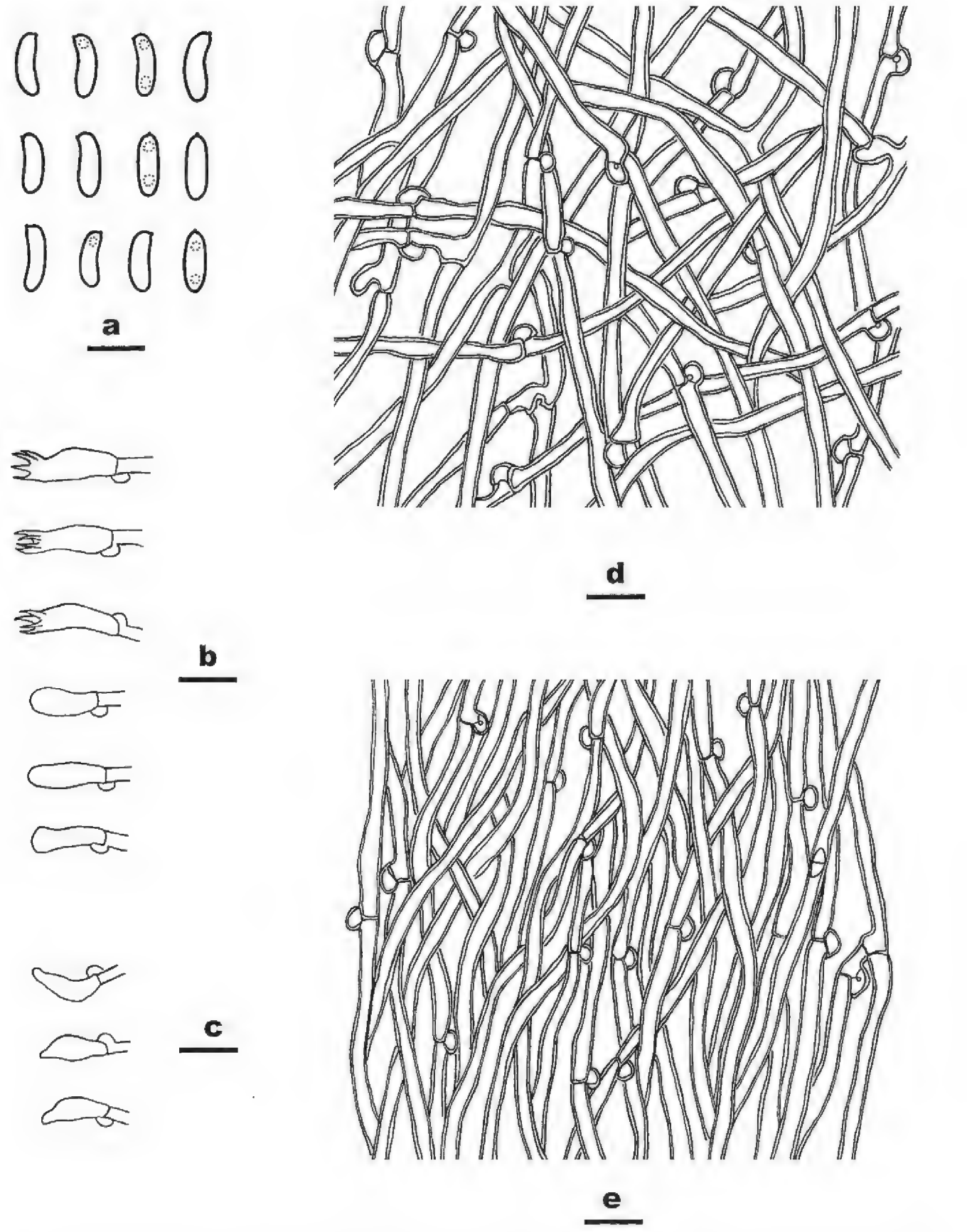

Figure 7. *Cyanosporus tabuliformis* (Dai 26063, holotype) **A** basidiospores **B** basidia and basidioles **C** cystidioles **D** hyphae from context **E** hyphae from trama. Scale bars: 5 μm (**A**); 10 μm (**B–E**).

Basidiospores cylindrical to allantoid, 4.3–5.5 × 1. 5–2 μm, L = 4.8 μm, W = 1.9 μm, Q = 2.6 (n = 60/2), hyaline, thin-walled, sometimes with one or two small guttules, IKI–, CB–.

Type of rot. Brown rot.

Additional specimen examined. CHINA. • Shanxi: Changzhi, Qinyuan County, Taiyueshan Forest Park, 31 Aug. 2023, on fallen branch of *Pinus tabuliformis*, Dai 26066 (BJFC 043615, Genbank: ITS PP479789, LSU PP479811, mtSSU PP510204, nrSSU PP488296, RPB1 PP526266, TEF1 PP526280).

Discussion

The *Cyanosporus* was established by McGinty in1909 with one species *C. caesius*. Recently, Papp (2014) based on morphological characters, proposed the subgenus *Postia* subg. *Cyanosporus* for the *P. caesius* complex. Mi-

ettinen et al. (2018) studied the *Postia caesia* complex using sequences from two DNA loci, ITS and TEF1 selected a neotype of *P. caesia* (LY BR-6776 collected from Germany) from type locality and described ten new species in *Postia*. However, *Cyanosporus* as an independent genus was raised again in recent studies (Shen et al. 2019; Liu et al. 2021, 2022, 2023). In our study, samples of 38 *Cyanosporus* species including three new species formed a strongly supported clade distinguished from *Postia* (Fig. 1).

Cyanosporus is a cosmopolitan genus causing a brown rot in different angiosperm and gymnosperm wood. Out of 38 species, currently 26 species are recorded in China. *Cyanosporus* usually has effused-reflexed to pileate poroid basidiomata with a bluish tint and thin- to slightly thick-walled basidiospores distinguished from other genera of Postiaceae (Liu et al. 2023).

Cyanosporus linzhiensis is phylogenetically related to *C. magnus* (Miettinen) B.K. Cui & Shun Liu, and both species have pileate basidiomata with white, velutinate and azonate pileal surface, almost the same size of pores (4–5 per mm in *C. magnus* vs. 5–6 per mm in *C. linzhiensis*, Miettinen et al. 2018), and they are recorded in China. However, the latter has distinct white pileal margin and narrower basidiospores (3.6–4.4 × 1–1.2 µm vs. 4–5 × 1.2–1.5 µm, Miettinen et al. 2018). *Cyanosporus caesiosimulans* and *C. livens* are similar to *C. linzhiensis* by white velutinate pileal surface, almost the same pores (5–7 per mm in *C. caesiosimulans*; 4–6 per mm in *C. livens*; 5–6 per mm in *C. linzhiensis*, Miettinen et al. 2018) and allantoid basidiospores of about the same size (4.2–5.5 × 1.1–1.4 µm in *C. caesiosimulans*; 4.1–5.7 × 1.1–1.5 µm in *C. livens*; 4–5 × 1.2–1.5 µm in *C. linzhiensis*, Miettinen et al. 2018). However, the former two are not currently distributed in China, and unrelated to *C. linzhiensis* in phylogeny.

Cyanosporus miscanthi and *C. rigidus* B.K. Cui & Shun Liu are phylogenetically related (Fig. 1), but they are different in morphology. The latter has rigid basidiomata when dry, buff yellow to clay buff and distinct concentrically zonate pileal surface when fresh, buff-yellow to pinkish buff pore surface when dry, the absence of cystidioles and smaller basidiospores (3.7–4.2 × 0.9–1.3 µm vs. 4–5 × 1.5–2 µm, Liu et al. 2022). *Cyanosporus nothofagicola* B.K. Cui, Shun Liu & Y.C. Dai, *C. tenuis* B.K. Cui, Shun Liu & Y.C. Dai and *C. miscanthi* share effused-reflexed to pileate basidiomata, soft corky to fragile when dry, angular pores, white, pale mouse gray to pale bluish gray pore surface when fresh, and fusoid cystidioles. However, *C. nothofagicola* has narrower basidiospores (3.8–5 × 1–1.7 µm vs. 4–5 × 1.5–2 µm, Liu et al. 2021), and is grown on *Nothofagus* occurring in Australia. *Cyanosporus tenuis* also has tiny basidiomata, but it has wider contextual hyphae (2.6–7 µm in diam. vs. 3–4.5 µm in diam.), larger basidia (18–28 × 3.7–6 µm vs. 9–13 × 4–5 µm) and relatively larger basidiospores (4.7–6 × 1.3–2 µm vs. 4–5 × 1.5–2 µm, Liu et al. 2021). In addition, they form independent lineages in the phylogeny (Fig. 1).

Cyanosporus tabuliformis and *C. auricomus* (Spirin & Niemelä) B.K. Cui & Shun Liu form a sister group without strong support. They share the pileate basidiomata with hirsute and azonate pileal surface, almost the same size of pores (4–6 per mm vs. 4–5 per mm, Miettinen et al. 2018) and basidiospores (4.4–5.6 × 1.5–1.8 µm vs. 4.3–5.5 × 1.5–2 µm, Miettinen et al. 2018), and growth on gymnosperm wood. However, the latter has bright yellow pore surface when fresh, green when bruised (Miettinen et al. 2018); moreover, their sister relationship lacks strong support hinting at them being two distinct species.

Cyanosporus cyanescens (Miettinen) B.K. Cui & Shun Liu has pileal surface with cream to pale ochraceous color at the base, grayish blue at the margin when fresh, and it is somewhat similar to *C. tabuliformis*, yet its slimmer basidiospores (4.7–6.1 × 1.1–1.6 µm vs. 4.3–5.5 × 1.5–2 µm, Miettinen et al. 2018) make it different from *C. tabuliformis*. In addition, *C. cyanescens* is distantly related to *C. tabuliformis* in our phylogeny (Fig. 1).

Although extensive studies on Chinese polypores have been carried out recently, and more than 1000 species were reported (Dai 2009; Cui et al. 2019; Dai et al. 2021; Wu et al. 2022a, 2022b; Mao et al. 2023; Wang et al. 2023; Yuan et al. 2023; Zhang et al. 2023; Zhou et al. 2023; Zhao et al. 2024), the richness of this group fungi is still not well recognized, especially in the southwest China. In this paper two species of *Cyanosporus* are described from Xizang (Tibet, southwest China) demonstrate that more taxa will be described after further investigations in the virgin forests of Xizang.

Acknowledgements

John McNeill (Royal Botanic Garden, Edinburgh) is thanked for his kind assistance on some of our nomenclature inquiries.

Additional information

Conflict of interest

The authors have declared that no competing interests exist.

Ethical statement

No ethical statement was reported.

Funding

The research is supported by the National Natural Science Foundation of China (Project Nos. 32161143013, 32370013), the Yunnan Province expert workstation program (No. 202205AF150014), and Iran National Science Foundation (No. 4000655).

Author contributions

Chao-Ge Wang, Shun Liu, Masoomeh Ghobad-Nejhad, Hong-Gao Liu, Yu-Cheng Dai and Yuan Yuan designed the research and contributed to data analysis and interpretation. Chao-Ge Wang and Shun Liu conducted the molecular experiments and analyzed the data. Chao-Ge Wang and Yu-Cheng Dai prepared the samples and drafted the manuscript. Chao-Ge Wang, Masoomeh Ghobad-Nejhad, Hong-Gao Liu, Yu-Cheng Dai and Yuan Yuan discussed the results and edited the manuscript. All authors contributed to the article and approved the submitted version.

Author ORCIDs

Chao-Ge Wang https://orcid.org/0000-0003-4381-5720
Shun Liu https://orcid.org/0000-0001-9261-4365
Masoomeh Ghobad-Nejhad https://orcid.org/0000-0002-7807-4187
Hong-Gao Liu https://orcid.org/0000-0002-9508-3245
Yu-Cheng Dai https://orcid.org/0000-0002-6523-0320
Yuan Yuan https://orcid.org/0000-0001-6674-9848

Data availability

All of the data that support the findings of this study are available in the main text.

References

Anonymous (1969) Flora of British fungi. Colour identification chart. Her Majesty's Stationery Office, London.

Capella-Gutierrez S, Silla-Martinez JM, Gabaldon T (2009) trimAl: A tool for automated alignment trimming in large-scale phylogenetic analyses. Bioinformatics (Oxford, England) 25(15): 1972–1973. https://doi.org/10.1093/bioinformatics/btp348

Corner EJH (1989) Ad Polyporaceas V. Beihefte zur Nova Hedwigia 96: 1–218.

Cui BK, Li HJ, Ji X, Zhou JL, Song J, Si J, Yang ZL, Dai YC (2019) Species diversity, taxonomy and phylogeny of Polyporaceae (Basidiomycota) in China. Fungal Diversity 97(1): 137–392. https://doi.org/10.1007/s13225-019-00427-4

Dai YC (2009) The checklist of Chinese polypores. Junwu Xuebao 28: 315–327. [in Chinese]

Dai YC, Yang ZL, Cui BK, Wu G, Yuan HS, Zhou LW, He SH, Ge ZW, Wu F, Wei YL, Yuan Y, Si J (2021) Diversity and systematics of the important macrofungi in Chinese forests. Junwu Xuebao 40: 770–805.

David A (1980) Étude du genre *Tyromyces* sensu lato: Répartition dans les genres *Leptoporus*, *Spongiporus* et *Tyromyces* sensu stricto. Bulletin Mensuel de la Societe Linneenne de Lyon 49(1): 6–56. https://doi.org/10.3406/linly.1980.10404

Donk MA (1960) The generic names proposed for Hymenomycetes – 10. The generic names proposed for Polyporaceae. Persoonia 1: 173–302.

Fries EM (1821). Systema Mycologicum. 1: 1–520.

Gilbertson RL, Ryvarden L (1985) Some new combinations in the Polyporaceae. Mycotaxon 22: 363–365.

Hall TA (1999) BioEdit: A user-friendly biological sequence alignment editor and analysis program for Windows 95/98/NT. Nucleic Acids Symposium Series 41: 95–98.

Han ML, Chen YY, Shen LL, Song J, Vlasák J, Dai YC, Cui BK (2016) Taxonomy and phylogeny of the brown-rot fungi: *Fomitopsis* and its related genera. Fungal Diversity 80(1): 343–373. https://doi.org/10.1007/s13225-016-0364-y

Hopple Jr JS, Vilgalys R (1999) Phylogenetic relationships in the mushroom genus *Coprinus* and dark-spored allies based on sequence data from the nuclear gene coding for the large ribosomal subunit RNA: Divergent domains, outgroups, and monophyly. Molecular Phylogenetics and Evolution 13(1): 1–19. https://doi.org/10.1006/mpev.1999.0634

Jahn H (1963) Mitteleuropäische Porlinge (Polyporaceae s. lato) und ihr Vorkommen in Westfalen. Westfälische Pilzbriefe 4: 1–143.

Jülich W (1982) Notes on some Basidiomycetes (Aphyllophorales and Heterobasidiomycetes). Persoonia 11: 421–428.

Katoh K, Standley DM (2013) MAFFT multiple sequence alignment software version 7: Improvements in performance and usability. Molecular Biology and Evolution 30(4): 772–780. https://doi.org/10.1093/molbev/mst010

Liu S, Shen LL, Wang Y, Xu TM, Gates G, Cui BK (2021) Species Diversity and Molecular Phylogeny of *Cyanosporus* (Polyporales, Basidiomycota). Frontiers in Microbiology 12: 631166. https://doi.org/10.3389/fmicb.2021.631166

Liu S, Xu TM, Song CG, Zhao CL, Wu DM, Cui BK (2022) Species diversity, molecular phylogeny and ecological habits of *Cyanosporus* (Polyporales, Basidiomycota) with an emphasis on Chinese collections. MycoKeys 86: 19–46. https://doi.org/10.3897/mycokeys.86.78305

Liu S, Chen YY, Sun YF, He XL, Song CG, Si J, Liu DM, Gates G, Cui BK (2023) Systematic classifcation and phylogenetic relationships of the brown-rot fungi within the Polyporales. Fungal Diversity 118(1): 1–94. https://doi.org/10.1007/s13225-022-00511-2

Lloyd CG (1909) Mycological Notes 33. Mycological Writings 3: 425–444.

Lowe JL (1975) Polyporaceae of North America. The genus *Tyromyces*. Mycotaxon 2: 1–82.

Maddison WP, Maddison DR (2017) Mesquite: A Modular System for Evolutionary Analysis, Version 3.2. http://mesquiteproject.org [accessed October 2020]

Mao WL, Wu YD, Liu HG, Yuan Y, Dai YC (2023) A contribution to *Porogramme* (Polyporaceae, Agaricomycetes) and related genera. IMA Fungus 14(1): 5. https://doi.org/10.1186/s43008-023-00110-z

Matheny PB (2005) Improving phylogenetic inference of mushrooms with RPB1 and RPB2 nucleotide sequences (*Inocybe*, Agaricales). Molecular Phylogenetics and Evolution 35(1): 1–20. https://doi.org/10.1016/j.ympev.2004.11.014

Matheny PB, Liu YJ, Ammirati JF, Hall BD (2002) Using RPB1 sequences to improve phylogenetic inference among mushrooms (*Inocybe*, Agaricales). American Journal of Botany 89(4): 688–698. https://doi.org/10.3732/ajb.89.4.688

Miettinen O, Vlasák J, Rivoire B, Spirin V (2018) *Postia caesia* complex (Polyporales, Basidiomycota) in temperate Northern Hemisphere. Fungal Systematics and Evolution 1(1): 101–129. https://doi.org/10.3114/fuse.2018.01.05

Miller MA, Pfeiffer W, Schwartz T (2010) "Creating the CIPRES Science Gateway for inference of large phylogenetic trees" in Proceedings of the Gateway Computing Environments Workshop (GCE), 14 Nov. 2010, New Orleans, 1–8. https://doi.org/10.1109/GCE.2010.567612 [Archived by WebCite at http://www.webcitation.org/5imQlJeQa]

Murrill WA (1907) Polyporaceae, Part 1. North American Flora 9: 1–72.

Niemelä T, Kinnunen J, Lindgren M, Manninen O, Miettinen O, Penttilä R, Turunen O (2001) Novelties and records of poroid Basidiomycetes in Finland and adjacent Russia. Karstenia 41(1): 1–21. https://doi.org/10.29203/ka.2001.373

Nylander JAA (2004) MrModeltest vol 2. Program distributed by the author. Evolutionary Biology Centre, Uppsala University.

Ortiz-Santana B, Lindner DL, Miettinen O, Justo A, Justo A, Hibbett DS (2013) A phylogenetic overview of the antrodia clade (Basidiomycota, Polyporales). Mycologia 105(6): 1391–1411. https://doi.org/10.3852/13-051

Papp V (2014) Nomenclatural novelties in the *Postia caesia* complex. Mycotaxon 129(2): 407–413. https://doi.org/10.5248/129.407

Petersen JH (1996) The Danish Mycological Society's colour-chart. Foreningen til Svampekundskabens Fremme, Greve.

Pildain MB, Rajchenberg M (2012) The phylogenetic disposition of *Postia* s.l. (Polyporales, Basidiomycota) from Patagonia, Argentina. Mycologia 105(2): 357–367. https://doi.org/10.3852/12-088

Rehner SA, Buckley E (2005) A Beauveria phylogeny inferred from nuclear ITS and EF1-alpha sequences: Evidence for cryptic diversification and links to *Cordyceps* teleomorphs. Mycologia 97: 84–98. https://doi.org/10.3852/mycologia.97.1.84

Ronquist F, Huelsenbeck JP (2003) MRBAYES 3: Bayesian phylogenetic inference under mixed models. Bioinformatics (Oxford, England) 19(12): 1572–1574. https://doi.org/10.1093/bioinformatics/btg180

Ryvarden L, Gilbertson RL (1994) European polypores. Part 2. Synopsis Fungorum 7: 394–743.

Ryvarden L, Melo I (2017) Poroid fungi of Europe, 2nd edition. Synopsis Fungorum 37: 1–431.

Shen LL, Wang M, Zhou JL, Xing JH, Cui BK, Dai YC (2019) Taxonomy and phylogeny of *Postia*. Multi-gene phylogeny and taxonomy of the brown-rot fungi: *Postia* (Polyporales, Basidiomycota) and related genera. Persoonia 42(1): 101–126. https://doi.org/10.3767/persoonia.2019.42.05

Sun YF, Costa-Rezende DH, Xing JH, Zhou JL, Zhang B, Gibertoni TB, Gates G, Glen M, Dai YC, Cui BK (2020) Multi-gene phylogeny and taxonomy of *Amauroderma* s.lat. (Ganodermataceae). Persoonia 44(1): 206–239. https://doi.org/10.3767/persoonia.2020.44.08

Swofford DL (2002) PAUP*: phylogenetic analysis using parsimony (*and other methods), version 4.0b10. Sinauer Associates, Sunderland, Massachusetts. https://doi.org/10.1002/0471650129.dob0522

Thompson JD, Gibson TJ, Plewniak F, Jeanmougin F, Higgins DG (1997) The Clustal_X windows interface: Flexible strategies for multiple sequence alignment aided by quality analysis tools. Nucleic Acids Research 25(24): 4876–4882. https://doi.org/10.1093/nar/25.24.4876

Ţura D, Spirin WA, Zmitrovich IV, Wasser SP, Nevo E (2008) Polypores new to Israel – 1: Genera *Ceriporiopsis*, *Postia* and *Skeletocutis*. Mycotaxon 103: 217–227.

Wang CG, Zhao H, Liu HG, Zeng GY, Yuan Y, Dai YC (2023) A multi-gene phylogeny clarifies species diversity, taxonomy, and divergence times of *Ceriporia* and other related genera in Irpicaceae (Polyporales, Basidiomycota). Mycosphere: Journal of Fungal Biology 14(1): 1665–1729. https://doi.org/10.5943/mycosphere/14/1/19

White TJ, Bruns T, Lee S, Taylor J (1990) Amplification and direct sequencing of fungal ribosomal RNA genes for phylogenetics. In: Innis MA, Gelfand DH, Sninsky JJ, 1White, JT (Eds) PCR Protocols: A Guide to Methods and Applications. Academic Press, San Diego, 315–322. https://doi.org/10.1016/B978-0-12-372180-8.50042-1

Wu F, Zhou LW, Vlasák J, Dai YC (2022a) Global diversity and systematics of Hymenochaetaceae with poroid hymenophore. Fungal Diversity 113(1): 1–192. https://doi.org/10.1007/s13225-021-00496-4

Wu F, Man XW, Tohtirjap A, Dai YC (2022b) A comparison of polypore funga and species composition in forest ecosystems of China, North America, and Europe. Forest Ecosystems 9: 100051. https://doi.org/10.1016/j.fecs.2022.100051

Yuan Y, Bian LS, Wu YD, Chen JJ, Wu F, Liu HG, Zeng GY, Dai YC (2023) Species diversity of pathogenic wood-rotting fungi (Agaricomycetes, Basidiomycota) in China. Mycology 14(3): 204–226. https://doi.org/10.1080/21501203.2023.2238779

Zhang QY, Liu HG, Papp V, Zhou M, Dai YC, Yuan Y (2023) New insights into the classification and evolution of *Favolaschia* (Agaricales, Basidiomycota) and its potential distribution, with descriptions of eight new species. Mycosphere: Journal of Fungal Biology 14(1): 777–814. https://doi.org/10.5943/mycosphere/14/1/10

Zhao H, Wu YD, Yang ZR, Liu HG, Wu F, Dai YC, Yuan Y (2024) Polypore funga and species diversity in tropical forest ecosystems of Africa, America and Asia, and a comparison with temperate and boreal regions of the Northern Hemisphere. Forest Ecosystems 11: 100200. https://doi.org/10.1016/j.fecs.2024.100200

Zhou M, Dai YC, Vlasák J, Liu HG, Yuan Y (2023) Updated systematics of *Trichaptum* s.l. (Hymenochaetales, Basidiomycota). Mycosphere: Journal of Fungal Biology 14(1): 815–917. https://doi.org/10.5943/mycosphere/14/1/11

Zhu L, Song J, Zhou JL, Si J, Cui BK (2019) Species diversity, phylogeny, divergence time and biogeography of the genus *Sanghuangporus* (Basidiomycota). Frontiers in Microbiology 10: 812. https://doi.org/10.3389/fmicb.2019.00812